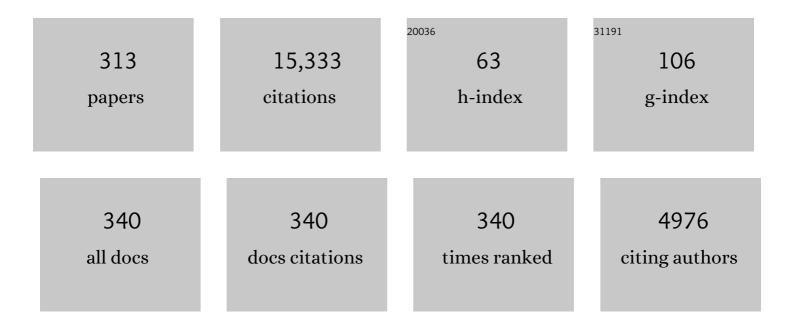
## **B J Anderson**

List of Publications by Year in descending order

Source: https://exaly.com/author-pdf/8398639/publications.pdf Version: 2024-02-01



RIANDERSON

#	Article	IF	CITATIONS
1	Investigation of the homogeneity of energy conversion processes at dipolarization fronts from MMS measurements. Physics of Plasmas, 2022, 29, .	0.7	5
2	Highâ€Latitude Electrodynamics Specified in SAMI3 Using AMPERE Fieldâ€Aligned Currents. Space Weather, 2022, 20, .	1.3	4
3	Distributions of Birkeland Current Density Observed by AMPERE are Heavyâ€Tailed or Longâ€Tailed. Journal of Geophysical Research: Space Physics, 2022, 127, .	0.8	4
4	Investigation of geomagnetic reference models based on the Iridium\$\$^{circledR }\$\$ constellation. Earth, Planets and Space, 2022, 74, .	0.9	4
5	lonospheric Energy Input in Response to Changes in Solar Wind Driving: Statistics From the SuperDARN and AMPERE Campaigns. Journal of Geophysical Research: Space Physics, 2022, 127, .	0.8	4
6	Occurrence Statistics of Horse Collar Aurora. Journal of Geophysical Research: Space Physics, 2022, 127, .	0.8	9
7	Influence of Off‣unâ€Earth Line Distance on the Accuracy of L1 Solar Wind Monitoring. Journal of Geophysical Research: Space Physics, 2022, 127, .	0.8	2
8	Lobe Reconnection and Cuspâ€Aligned Auroral Arcs. Journal of Geophysical Research: Space Physics, 2022, 127, .	0.8	11
9	Magnetosphereâ€lonosphere Coupling via Prescribed Fieldâ€Aligned Current Simulated by the TIEGCM. Journal of Geophysical Research: Space Physics, 2021, 126, .	0.8	8
10	Magnetospheric Flux Throughput in the Dungey Cycle: Identification of Convection State During 2010. Journal of Geophysical Research: Space Physics, 2021, 126, e2020JA028437.	0.8	26
11	Solar flare effects in the Earth's magnetosphere. Nature Physics, 2021, 17, 807-812.	6.5	27
12	Determining EMIC Wave Vector Properties Through Multiâ€Point Measurements: The Wave Curl Analysis. Journal of Geophysical Research: Space Physics, 2021, 126, e2020JA028922.	0.8	10
13	Determination of Auroral Electrodynamic Parameters From AMPERE Fieldâ€Aligned Current Measurements. Space Weather, 2021, 19, e2020SW002677.	1.3	14
14	MMS Observations of Field Line Resonances Under Disturbed Solar Wind Conditions. Journal of Geophysical Research: Space Physics, 2021, 126, e2020JA028936.	0.8	2
15	The Relationship Between Large Scale Thermospheric Density Enhancements and the Spatial Distribution of Poynting Flux. Journal of Geophysical Research: Space Physics, 2021, 126, e2021JA029205.	0.8	11
16	Iridium Communications Satellite Constellation Data for Study of Earth's Magnetic Field. Geochemistry, Geophysics, Geosystems, 2021, 22, e2020GC009515.	1.0	9
17	An Examination of Magnetosphereâ€lonosphere Influences During a SAPS Event. Geophysical Research Letters, 2021, 48, e2021GL095751.	1.5	4
18	The Role of Diffuse Electron Precipitation in the Formation of Subauroral Polarization Streams. Journal of Geophysical Research: Space Physics, 2021, 126, .	0.8	19

#	Article	IF	CITATIONS
19	Fieldâ€Aligned Current During an Interval of B <sub><i>Y</i></sub> â€Dominated Interplanetaryâ€Field; Modeledâ€toâ€Observed Comparisons. Journal of Geophysical Research: Space Physics, 2021, 126, .	0.8	0
20	A Third Generation Fieldâ€Aligned Current Model. Journal of Geophysical Research: Space Physics, 2020, 125, e2019JA027249.	0.8	7
21	Dayside Polar Cap Density Enhancements Formed During Substorms. Journal of Geophysical Research: Space Physics, 2020, 125, e2020JA028101.	0.8	2
22	An Improved Estimation of SuperDARN Heppnerâ€Maynard Boundaries Using AMPERE Data. Journal of Geophysical Research: Space Physics, 2020, 125, e2019JA027218.	0.8	9
23	The Evolution of Longâ€Duration Cusp Spot Emission During Lobe Reconnection With Respect to Fieldâ€Aligned Currents. Journal of Geophysical Research: Space Physics, 2020, 125, e2020JA027922.	0.8	13
24	Dualâ€Lobe Reconnection and Horseâ€Collar Auroras. Journal of Geophysical Research: Space Physics, 2020, 125, e2020JA028567.	0.8	21
25	A Deep Learningâ€Based Approach for Modeling the Dynamics of AMPERE Birkeland Currents. Journal of Geophysical Research: Space Physics, 2020, 125, e2020JA027908.	0.8	7
26	The BepiColombo–Mio Magnetometer en Route to Mercury. Space Science Reviews, 2020, 216, 1.	3.7	19
27	Heightâ€Integrated Ionospheric Conductances Parameterized By Interplanetary Magnetic Field and Substorm Phase. Journal of Geophysical Research: Space Physics, 2020, 125, e2020JA028121.	0.8	10
28	Conductance Model for Extreme Events: Impact of Auroral Conductance on Space Weather Forecasts. Space Weather, 2020, 18, e2020SW002551.	1.3	24
29	The Shape of Mercury's Magnetopause: The Picture From MESSENGER Magnetometer Observations and Future Prospects for BepiColombo. Journal of Geophysical Research: Space Physics, 2020, 125, e2019JA027544.	0.8	20
30	AMPERE polar cap boundaries. Annales Geophysicae, 2020, 38, 481-490.	0.6	14
31	Event Studies of Highâ€Latitude FACs With Inverse and Assimilative Analysis of AMPERE Magnetometer Data. Journal of Geophysical Research: Space Physics, 2020, 125, e2019JA027266.	0.8	3
32	Statistical Relations Between Auroral Electrical Conductances and Fieldâ€Aligned Currents at High Latitudes. Journal of Geophysical Research: Space Physics, 2020, 125, e2020JA028008.	0.8	16
33	Observations of Extreme ICME Ram Pressure Compressing Mercury's Dayside Magnetosphere to the Surface. Astrophysical Journal, 2020, 889, 184.	1.6	22
34	Modes of (FACs) Variability and Their Hemispheric Asymmetry Revealed by Inverse and Assimilative Analysis of Iridium Magnetometer Data. Journal of Geophysical Research: Space Physics, 2020, 125, e2019JA027265.	0.8	13
35	Bifurcated Region 2 Fieldâ€Aligned Currents Associated With Substorms. Journal of Geophysical Research: Space Physics, 2020, 125, e2019JA027041.	0.8	7
36	On the magnetic characteristics of magnetic holes in the solar wind between Mercury and Venus. Annales Geophysicae, 2020, 38, 51-60.	0.6	26

#	Article	IF	CITATIONS
37	Science Data Products for AMPERE. , 2020, , 141-165.		28
38	Spatial and Temporal Evolution of Different‣cale Ionospheric Irregularities in Central and East Siberia During the 27–28 May 2017 Geomagnetic Storm. Space Weather, 2020, 18, e2019SW002378.	1.3	6
39	Magnetometer in-flight offset accuracy for the BepiColombo spacecraft. Annales Geophysicae, 2020, 38, 823-832.	0.6	7
40	Investigation of Massâ€∤Chargeâ€Dependent Escape of Energetic Ions Across the Magnetopauses of Earth and Jupiter. Journal of Geophysical Research: Space Physics, 2019, 124, 5539-5567.	0.8	15
41	Timescales of Birkeland Currents Driven by the IMF. Geophysical Research Letters, 2019, 46, 7893-7901.	1.5	17
42	Highâ€Resolution Measurements of the Crossâ€Shock Potential, Ion Reflection, and Electron Heating at an Interplanetary Shock by MMS. Journal of Geophysical Research: Space Physics, 2019, 124, 3961-3978.	0.8	36
43	EMIC Waves in the Outer Magnetosphere: Observations of an Offâ€Equator Source Region. Geophysical Research Letters, 2019, 46, 5707-5716.	1.5	29
44	Substorm Onset Latitude and the Steadiness of Magnetospheric Convection. Journal of Geophysical Research: Space Physics, 2019, 124, 1738-1752.	0.8	17
45	Effects of Nearly Frontal and Highly Inclined Interplanetary Shocks on High‣atitude Fieldâ€Aligned Currents (FACs). Space Weather, 2019, 17, 1659-1673.	1.3	9
46	The Properties of Lion Roars and Electron Dynamics in Mirror Mode Waves Observed by the Magnetospheric MultiScale Mission. Journal of Geophysical Research: Space Physics, 2018, 123, 93-103.	0.8	26
47	MMS Observation of Shockâ€Reflected He <sup>++</sup> at Earth's Quasiâ€Perpendicular Bow Shock. Geophysical Research Letters, 2018, 45, 49-55.	1.5	11
48	Relation of Fieldâ€Aligned Currents Measured by the Network of Iridium® Spacecraft to Solar Wind and Substorms. Geophysical Research Letters, 2018, 45, 2151-2158.	1.5	9
49	Seasonal and Temporal Variations of Fieldâ€Aligned Currents and Ground Magnetic Deflections During Substorms. Journal of Geophysical Research: Space Physics, 2018, 123, 2696-2713.	0.8	19
50	Multiscale Currents Observed by MMS in the Flow Braking Region. Journal of Geophysical Research: Space Physics, 2018, 123, 1260-1278.	0.8	32
51	Magnetosphereâ€lonosphere Connection of Stormâ€Time Regionâ€2 Fieldâ€Aligned Current and Ring Current: Arase and AMPERE Observations. Journal of Geophysical Research: Space Physics, 2018, 123, 9545-9559.	0.8	7
52	The MESSENGER Mission: Science and Implementation Overview. , 2018, , 1-29.		10
53	The Chemical Composition of Mercury. , 2018, , 30-51.		43
54	Mercury's Crust and Lithosphere: Structure and Mechanics. , 2018, , 52-84.		9

0

#	Article	IF	CITATIONS
55	Mercury's Internal Structure. , 2018, , 85-113.		26
56	Mercury's Internal Magnetic Field. , 2018, , 114-143.		12
57	The Geologic History of Mercury. , 2018, , 144-175.		10
58	The Geochemical and Mineralogical Diversity of Mercury. , 2018, , 176-190.		21
59	Spectral Reflectance Constraints on the Composition and Evolution of Mercury's Surface. , 2018, , 191-216.		9
60	Impact Cratering of Mercury. , 2018, , 217-248.		10
61	The Tectonic Character of Mercury. , 2018, , 249-286.		16
62	The Volcanic Character of Mercury. , 2018, , 287-323.		13
63	Mercury's Hollows. , 2018, , 324-345.		12
64	Mercury's Polar Deposits. , 2018, , 346-370.		9
65	Observations of Mercury's Exosphere: Composition and Structure. , 2018, , 371-406.		5
66	Understanding Mercury's Exosphere: Models Derived from MESSENGER Observations. , 2018, , 407-429.		8
67	Structure and Configuration of Mercury's Magnetosphere. , 2018, , 430-460.		7
68	Mercury's Dynamic Magnetosphere. , 2018, , 461-496.		8
69	The Elusive Origin of Mercury. , 2018, , 497-515.		21
70	Mercury's Global Evolution. , 2018, , 516-543.		8
71	Future Missions: Mercury after MESSENGER. , 2018, , 544-569.		3

72 Index of Place Names. , 2018, , 582-584.

#	Article	IF	CITATIONS
73	MMS, Van Allen Probes, GOES 13, and Groundâ€Based Magnetometer Observations of EMIC Wave Events Before, During, and After a Modest Interplanetary Shock. Journal of Geophysical Research: Space Physics, 2018, 123, 8331-8357.	0.8	30
74	Dawnside Wedge Current System Formed During Intense Geomagnetic Storms. Journal of Geophysical Research: Space Physics, 2018, 123, 9093-9109.	0.8	14
75	The Association of High‣atitude Dayside Aurora With NBZ Fieldâ€Aligned Currents. Journal of Geophysical Research: Space Physics, 2018, 123, 3637-3645.	0.8	20
76	Temporal and Spatial Development of Global Birkeland Currents. Journal of Geophysical Research: Space Physics, 2018, 123, 4785-4808.	0.8	22
77	Swirl mission concept: Unraveling the enigma. Planetary and Space Science, 2018, 162, 73-88.	0.9	1
78	Magnetosphere dynamics during the 14ÂNovember 2012 storm inferred from TWINS, AMPERE, Van Allen Probes, and BATS-R-US–CRCM. Annales Geophysicae, 2018, 36, 107-124.	0.6	8
79	Statistical Relations Between Fieldâ€Aligned Currents and Precipitating Electron Energy Flux. Geophysical Research Letters, 2018, 45, 8738-8745.	1.5	9
80	Timescales of Dayside and Nightside Fieldâ€Aligned Current Response to Changes in Solar Windâ€Magnetosphere Coupling. Journal of Geophysical Research: Space Physics, 2018, 123, 7307-7319.	0.8	16
81	Overview of Solar Wind–Magnetosphere–Ionosphere–Atmosphere Coupling and the Generation of Magnetospheric Currents. Space Sciences Series of ISSI, 2018, , 555-581.	0.0	0
82	Exploring predictive performance: A reanalysis of the geospace model transition challenge. Space Weather, 2017, 15, 192-203.	1.3	33
83	Magnetospheric Multiscale Observations of Electron Vortex Magnetic Hole in the Turbulent Magnetosheath Plasma. Astrophysical Journal Letters, 2017, 836, L27.	3.0	85
84	Electron Heating at Kinetic Scales in Magnetosheath Turbulence. Astrophysical Journal, 2017, 836, 247.	1.6	50
85	Geomagnetically induced currents: Science, engineering, and applications readiness. Space Weather, 2017, 15, 828-856.	1.3	149
86	A comparison of smallâ€scale magnetic fluctuations in the Region 1 and 2 fieldâ€aligned current systems. Journal of Geophysical Research: Space Physics, 2017, 122, 3277-3290.	0.8	5
87	Birkeland currents during substorms: Statistical evidence for intensification of Regions 1 and 2 currents after onset and a localized signature of auroral dimming. Journal of Geophysical Research: Space Physics, 2017, 122, 6455-6468.	0.8	21
88	Global observations of magnetospheric highâ€ <i>m</i> poloidal waves during the 22 June 2015 magnetic storm. Geophysical Research Letters, 2017, 44, 3456-3464.	1.5	43
89	Structure, force balance, and topology of Earth's magnetopause. Science, 2017, 356, 960-963.	6.0	10
90	Comparison of predictive estimates of highâ€latitude electrodynamics with observations of globalâ€scale Birkeland currents. Space Weather, 2017, 15, 352-373.	1.3	35

#	Article	IF	CITATIONS
91	Magnetospheric Ion Evolution Across the Low‣atitude Boundary Layer Separatrix. Journal of Geophysical Research: Space Physics, 2017, 122, 10,247.	0.8	18
92	Lower Hybrid Drift Waves and Electromagnetic Electron Spaceâ€Phase Holes Associated With Dipolarization Fronts and Fieldâ€Aligned Currents Observed by the Magnetospheric Multiscale Mission During a Substorm. Journal of Geophysical Research: Space Physics, 2017, 122, 12,236.	0.8	31
93	Dominance of highâ€energy (>150ÂkeV) heavy ion intensities in Earth's middle to outer magnetosphere. Journal of Geophysical Research: Space Physics, 2017, 122, 9282-9293.	0.8	18
94	A Dynamic Model of Mercury's Magnetospheric Magnetic Field. Geophysical Research Letters, 2017, 44, 10147-10154.	1.5	30
95	Modeling observations of solar coronal mass ejections with heliospheric imagers verified with the Heliophysics System Observatory. Space Weather, 2017, 15, 955-970.	1.3	65
96	Statistical analysis of MMS observations of energetic electron escape observed at/beyond the dayside magnetopause. Journal of Geophysical Research: Space Physics, 2017, 122, 9440-9463.	0.8	14
97	The Effect of a Guide Field on Local Energy Conversion During Asymmetric Magnetic Reconnection: Particleâ€inâ€Cell Simulations. Journal of Geophysical Research: Space Physics, 2017, 122, 11,523.	0.8	27
98	Overview of Solar Wind–Magnetosphere–Ionosphere–Atmosphere Coupling and the Generation of Magnetospheric Currents. Space Science Reviews, 2017, 206, 547-573.	3.7	105
99	Near-Earth plasma sheet boundary dynamics during substorm dipolarization. Earth, Planets and Space, 2017, 69, 129.	0.9	15
100	Optimized merging of search coil and fluxgate data for MMS. Geoscientific Instrumentation, Methods and Data Systems, 2016, 5, 521-530.	0.6	22
101	Magnetopause erosion during the 17 March 2015 magnetic storm: Combined fieldâ€aligned currents, auroral oval, and magnetopause observations. Geophysical Research Letters, 2016, 43, 2396-2404.	1.5	36
102	MESSENGER observations of induced magnetic fields in Mercury's core. Geophysical Research Letters, 2016, 43, 2436-2444.	1.5	51
103	Seasonal and diurnal variations in AMPERE observations of the Birkeland currents compared to modeled results. Journal of Geophysical Research: Space Physics, 2016, 121, 4027-4040.	0.8	76
104	MESSENGER observations of cusp plasma filaments at Mercury. Journal of Geophysical Research: Space Physics, 2016, 121, 8260-8285.	0.8	29
105	Observations of energetic particle escape at the magnetopause: Early results from the MMS Energetic Ion Spectrometer (EIS). Geophysical Research Letters, 2016, 43, 5960-5968.	1.5	23
106	Modeling magnetospheric energetic particle escape across Earth's magnetopause as observed by the MMS mission. Geophysical Research Letters, 2016, 43, 4081-4088.	1.5	19
107	Wave telescope technique for MMS magnetometer. Geophysical Research Letters, 2016, 43, 4774-4780.	1.5	15
108	Steepening of waves at the duskside magnetopause. Geophysical Research Letters, 2016, 43, 7373-7380.	1.5	14

#	Article	IF	CITATIONS
109	Data assimilation of lowâ€altitude magnetic perturbations into a global magnetosphere model. Space Weather, 2016, 14, 165-184.	1.3	22
110	MMS observations of ionâ€scale magnetic island in the magnetosheath turbulent plasma. Geophysical Research Letters, 2016, 43, 7850-7858.	1.5	53
111	Multispacecraft observations and modeling of the 22/23 June 2015 geomagnetic storm. Geophysical Research Letters, 2016, 43, 7311-7318.	1.5	27
112	Force balance at the magnetopause determined with MMS: Application to flux transfer events. Geophysical Research Letters, 2016, 43, 11,941.	1.5	27
113	The 17 March 2013 storm: Synergy of observations related to electric field modes and their ionospheric and magnetospheric Effects. Journal of Geophysical Research: Space Physics, 2016, 121, 10,880.	0.8	27
114	Multispacecraft analysis of dipolarization fronts and associated whistler wave emissions using MMS data. Geophysical Research Letters, 2016, 43, 7279-7286.	1.5	49
115	A comparative study of dipolarization fronts at MMS and Cluster. Geophysical Research Letters, 2016, 43, 6012-6019.	1.5	37
116	Electrodynamic context of magnetopause dynamics observed by magnetospheric multiscale. Geophysical Research Letters, 2016, 43, 5988-5996.	1.5	10
117	Whistler mode waves and Hall fields detected by MMS during a dayside magnetopause crossing. Geophysical Research Letters, 2016, 43, 5943-5952.	1.5	44
118	The permeability of the magnetopause to a multispecies substorm injection of energetic particles. Geophysical Research Letters, 2016, 43, 9453-9460.	1.5	7
119	Dipolarization in the inner magnetosphere during a geomagnetic storm on 7 October 2015. Geophysical Research Letters, 2016, 43, 9397-9405.	1.5	7
120	MESSENGER observations of suprathermal electrons in Mercury's magnetosphere. Geophysical Research Letters, 2016, 43, 550-555.	1.5	35
121	Average fieldâ€aligned current configuration parameterized by solar wind conditions. Journal of Geophysical Research: Space Physics, 2016, 121, 1294-1307.	0.8	45
122	The FIELDS Instrument Suite on MMS: Scientific Objectives, Measurements, and Data Products. Space Science Reviews, 2016, 199, 105-135.	3.7	390
123	The Magnetospheric Multiscale Magnetometers. Space Science Reviews, 2016, 199, 189-256.	3.7	896
124	LONGITUDINAL PROPERTIES OF A WIDESPREAD SOLAR ENERGETIC PARTICLE EVENT ON 2014 FEBRUARY 25: EVOLUTION OF THE ASSOCIATED CME SHOCK. Astrophysical Journal, 2016, 819, 72.	1.6	72
125	The Magnetospheric Multiscale Magnetometers. , 2016, 199, 189.		1
126	MESSENGER observations of magnetospheric substorm activity in Mercury's near magnetotail. Geophysical Research Letters, 2015, 42, 3692-3699.	1.5	50

#	Article	IF	CITATIONS
127	First observations of Mercury's plasma mantle by MESSENGER. Geophysical Research Letters, 2015, 42, 9666-9675.	1.5	29
128	Improving solar wind modeling at Mercury: Incorporating transient solar phenomena into the WSAâ€ENLIL model with the Cone extension. Journal of Geophysical Research: Space Physics, 2015, 120, 5667-5685.	0.8	16
129	Interplanetary coronal mass ejections from MESSENGER orbital observations at Mercury. Journal of Geophysical Research: Space Physics, 2015, 120, 6101-6118.	0.8	88
130	MESSENGER observations of solar energetic electrons within Mercury's magnetosphere. Journal of Geophysical Research: Space Physics, 2015, 120, 8559-8571.	0.8	16
131	On the formation and origin of substorm growth phase/onset auroral arcs inferred from conjugate spaceâ€ground observations. Journal of Geophysical Research: Space Physics, 2015, 120, 8707-8722.	0.8	21
132	Dominant modes of variability in largeâ€scale Birkeland currents. Journal of Geophysical Research: Space Physics, 2015, 120, 6722-6735.	0.8	22
133	Birkeland current effects on highâ€ <b>ł</b> atitude ground magnetic field perturbations. Geophysical Research Letters, 2015, 42, 7248-7254.	1.5	29
134	MESSENGER observations of multiscale Kelvinâ€Helmholtz vortices at Mercury. Journal of Geophysical Research: Space Physics, 2015, 120, 4354-4368.	0.8	40
135	Interpreting ~1 Hz magnetic compressional waves in Mercury's inner magnetosphere in terms of propagating ionâ€Bernstein waves. Journal of Geophysical Research: Space Physics, 2015, 120, 4213-4228.	0.8	21
136	Modular model for Mercury's magnetospheric magnetic field confined within the average observed magnetopause. Journal of Geophysical Research: Space Physics, 2015, 120, 4503-4518.	0.8	59
137	Inverse procedure for high″atitude ionospheric electrodynamics: Analysis of satelliteâ€borne magnetometer data. Journal of Geophysical Research: Space Physics, 2015, 120, 5241-5251.	0.8	22
138	Principal component analysis of Birkeland currents determined by the Active Magnetosphere and Planetary Electrodynamics Response Experiment. Journal of Geophysical Research: Space Physics, 2015, 120, 10,415.	0.8	38
139	Comprehensive survey of energetic electron events in Mercury's magnetosphere with data from the MESSENGER Gammaâ€Ray and Neutron Spectrometer. Journal of Geophysical Research: Space Physics, 2015, 120, 2851-2876.	0.8	36
140	MESSENGER observations of flux ropes in Mercury's magnetotail. Planetary and Space Science, 2015, 115, 77-89.	0.9	71
141	Low-altitude magnetic field measurements by MESSENGER reveal Mercury's ancient crustal field. Science, 2015, 348, 892-895.	6.0	89
142	Constraints on the secular variation of Mercury's magnetic field from the combined analysis of MESSENGER and Mariner 10 data. Geophysical Research Letters, 2014, 41, 6627-6634.	1.5	23
143	Event study combining magnetospheric and ionospheric perspectives of the substorm current wedge modeling. Journal of Geophysical Research: Space Physics, 2014, 119, 9714-9728.	0.8	15
144	The magnitudes of the regions 1 and 2 Birkeland currents observed by AMPERE and their role in solar windâ€magnetosphereâ€ionosphere coupling. Journal of Geophysical Research: Space Physics, 2014, 119, 9804-9815.	0.8	56

#	Article	IF	CITATIONS
145	Global ionospheric and thermospheric response to the 5 April 2010 geomagnetic storm: An integrated dataâ€model investigation. Journal of Geophysical Research: Space Physics, 2014, 119, 10,358.	0.8	46
146	Development of large-scale Birkeland currents determined from the Active Magnetosphere and Planetary Electrodynamics Response Experiment. Geophysical Research Letters, 2014, 41, 3017-3025.	1.5	156
147	Statistical relationship between largeâ€scale upward fieldâ€eligned currents and electron precipitation. Journal of Geophysical Research: Space Physics, 2014, 119, 6715-6731.	0.8	58
148	Electric currents of a substorm current wedge on 24 February 2010. Geophysical Research Letters, 2014, 41, 4449-4455.	1.5	17
149	lon kinetic properties in Mercury's preâ€midnight plasma sheet. Geophysical Research Letters, 2014, 41, 5740-5747.	1.5	50
150	MESSENGER at Mercury: Early orbital operations. Acta Astronautica, 2014, 93, 509-515.	1.7	4
151	Structure and dynamics of Mercury's magnetospheric cusp: MESSENGER measurements of protons and planetary ions. Journal of Geophysical Research: Space Physics, 2014, 119, 6587-6602.	0.8	79
152	Steadyâ€state fieldâ€aligned currents at Mercury. Geophysical Research Letters, 2014, 41, 7444-7452.	1.5	55
153	MESSENGER observations of large dayside flux transfer events: Do they drive Mercury's substorm cycle?. Journal of Geophysical Research: Space Physics, 2014, 119, 5613-5623.	0.8	54
154	Active current sheets and candidate hot flow anomalies upstream of Mercury's bow shock. Journal of Geophysical Research: Space Physics, 2014, 119, 853-876.	0.8	22
155	Comparison of magnetic perturbation data from LEO satellite constellations: Statistics of DMSP and AMPERE. Space Weather, 2014, 12, 2-23.	1.3	33
156	Plasma distribution in Mercury's magnetosphere derived from MESSENGER Magnetometer and Fast Imaging Plasma Spectrometer observations. Journal of Geophysical Research: Space Physics, 2014, 119, 2917-2932.	0.8	46
157	Mercury's surface magnetic field determined from protonâ€reflection magnetometry. Geophysical Research Letters, 2014, 41, 4463-4470.	1.5	39
158	MESSENGER observations of Mercury's dayside magnetosphere under extreme solar wind conditions. Journal of Geophysical Research: Space Physics, 2014, 119, 8087-8116.	0.8	125
159	A superposed epoch analysis of the regions 1 and 2 Birkeland currents observed by AMPERE during substorms. Journal of Geophysical Research: Space Physics, 2014, 119, 9834-9846.	0.8	48
160	Temporal and spatial dynamics of the regions 1 and 2 Birkeland currents during substorms. Journal of Geophysical Research: Space Physics, 2013, 118, 3007-3016.	0.8	52
161	On the influence of open magnetic flux on substorm intensity: Ground―and spaceâ€based observations. Journal of Geophysical Research: Space Physics, 2013, 118, 2958-2969.	0.8	35
162	Global evolution of Birkeland currents on 10 min timescales: MHD simulations and observations. Journal of Geophysical Research: Space Physics, 2013, 118, 4977-4997.	0.8	31

#	Article	IF	CITATIONS
163	Empirical reconstruction of storm time steady magnetospheric convection events. Journal of Geophysical Research: Space Physics, 2013, 118, 6434-6456.	0.8	29
164	ULF Signals Observed Near the Magnetopause. Geophysical Monograph Series, 2013, , 269-276.	0.1	15
165	Upstream ultraâ€low frequency waves in Mercury's foreshock region: MESSENGER magnetic field observations. Journal of Geophysical Research: Space Physics, 2013, 118, 2809-2823.	0.8	40
166	Magnetic flux pileup and plasma depletion in Mercury's subsolar magnetosheath. Journal of Geophysical Research: Space Physics, 2013, 118, 7181-7199.	0.8	96
167	Cyclic reformation of a quasiâ€parallel bow shock at Mercury: MESSENGER observations. Journal of Geophysical Research: Space Physics, 2013, 118, 6457-6464.	0.8	25
168	A comparison of magnetic overshoots at the bow shocks of Mercury and Saturn. Journal of Geophysical Research: Space Physics, 2013, 118, 4381-4390.	0.8	17
169	Distribution and compositional variations of plasma ions in Mercury's space environment: The first three Mercury years of MESSENGER observations. Journal of Geophysical Research: Space Physics, 2013, 118, 1604-1619.	0.8	85
170	Mercury's magnetopause and bow shock from MESSENGER Magnetometer observations. Journal of Geophysical Research: Space Physics, 2013, 118, 2213-2227.	0.8	182
171	Auroral Current and Electrodynamics Structure (ACES) observations of ionospheric feedback in the Alfvén resonator and model responses. Journal of Geophysical Research: Space Physics, 2013, 118, 3288-3296.	0.8	19
172	MESSENGER observations of magnetopause structure and dynamics at Mercury. Journal of Geophysical Research: Space Physics, 2013, 118, 997-1008.	0.8	141
173	A magnetic disturbance index for Mercury's magnetic field derived from MESSENGER Magnetometer data. Geochemistry, Geophysics, Geosystems, 2013, 14, 3875-3886.	1.0	39
174	Fieldâ€aligned current reconfiguration and magnetospheric response to an impulse in the interplanetary magnetic field <i>B</i> <sub>Y</sub> component. Geophysical Research Letters, 2013, 40, 2489-2494.	1.5	10
175	Intense solar nearâ€relativistic electron events at 0.3 AU. Journal of Geophysical Research: Space Physics, 2013, 118, 63-73.	0.8	13
176	The detailed spatial structure of fieldâ€aligned currents comprising the substorm current wedge. Journal of Geophysical Research: Space Physics, 2013, 118, 7714-7727.	0.8	63
177	An Overview of Spacecraft Observations of 10 s to 600 s Period Magnetic Pulsations in the Earth's Magnetosphere. Geophysical Monograph Series, 2013, , 25-43.	0.1	30
178	Current Closure in the Auroral Ionosphere: Results From the Auroral Current and Electrodynamics Structure Rocket Mission. Geophysical Monograph Series, 2013, , 183-192.	0.1	6
179	Reduction in fieldâ€aligned currents preceding and local to auroral substorm onset. Geophysical Research Letters, 2012, 39, .	1.5	24
180	MESSENGER observations of dipolarization events in Mercury's magnetotail. Journal of Geophysical Research, 2012, 117, .	3.3	72

#	Article	IF	CITATIONS
181	Spatial distribution and spectral characteristics of energetic electrons in Mercury's magnetosphere. Journal of Geophysical Research, 2012, 117, .	3.3	28
182	MULTI-POINT SHOCK AND FLUX ROPE ANALYSIS OF MULTIPLE INTERPLANETARY CORONAL MASS EJECTIONS AROUND 2010 AUGUST 1 IN THE INNER HELIOSPHERE. Astrophysical Journal, 2012, 758, 10.	1.6	109
183	Survey of coherent â^1⁄41 Hz waves in Mercury's inner magnetosphere from MESSENGER observations. Journal of Geophysical Research, 2012, 117, .	3.3	39
184	MESSENGER observations of a fluxâ€ŧransferâ€event shower at Mercury. Journal of Geophysical Research, 2012, 117, .	3.3	85
185	Characteristics of the plasma distribution in Mercury's equatorial magnetosphere derived from MESSENGER Magnetometer observations. Journal of Geophysical Research, 2012, 117, .	3.3	23
186	Solar wind alpha particles and heavy ions in the inner heliosphere observed with MESSENGER. Journal of Geophysical Research, 2012, 117, .	3.3	54
187	Io Volcano Observer's (IVO) integrated approach to optimizing system design for radiation challenges. , 2012, , .		3
188	MESSENGER at Mercury: A mid-term report. Acta Astronautica, 2012, 81, 369-379.	1.7	13
189	MESSENGER and Mariner 10 flyby observations of magnetotail structure and dynamics at Mercury. Journal of Geophysical Research, 2012, 117, .	3.3	86
190	MESSENGER orbital observations of largeâ€amplitude Kelvinâ€Helmholtz waves at Mercury's magnetopause. Journal of Geophysical Research, 2012, 117, .	3.3	69
191	Forcing the TIEGCM model with Birkeland currents from the Active Magnetosphere and Planetary Electrodynamics Response Experiment. Journal of Geophysical Research, 2012, 117, .	3.3	24
192	Observations of Mercury's northern cusp region with MESSENGER's Magnetometer. Geophysical Research Letters, 2012, 39, .	1.5	86
193	Lowâ€degree structure in Mercury's planetary magnetic field. Journal of Geophysical Research, 2012, 117,	3.3	131
194	MESSENGER observations of Mercury's magnetic field structure. Journal of Geophysical Research, 2012, 117, .	3.3	109
195	Intense dayside Joule heating during the 5 April 2010 geomagnetic storm recovery phase observed by AMIE and AMPERE. Journal of Geophysical Research, 2012, 117, .	3.3	25
196	Dynamics of the region 1 Birkeland current oval derived from the Active Magnetosphere and Planetary Electrodynamics Response Experiment (AMPERE). Journal of Geophysical Research, 2012, 117, .	3.3	75
197	Remote and in situ observations of an unusual Earthâ€directed coronal mass ejection from multiple viewpoints. Journal of Geophysical Research, 2012, 117, .	3.3	86
198	The Radial Variation of Interplanetary Shocks in the Inner Heliosphere: Observations by Helios, MESSENGER, and STEREO. Solar Physics, 2012, 278, 421-433.	1.0	10

#	Article	IF	CITATIONS
199	Plasma pressure in Mercury's equatorial magnetosphere derived from MESSENGER Magnetometer observations. Geophysical Research Letters, 2011, 38, n/a-n/a.	1.5	38
200	Quasi-trapped ion and electron populations at Mercury. Geophysical Research Letters, 2011, 38, n/a-n/a.	1.5	40
201	Kinetic-scale magnetic turbulence and finite Larmor radius effects at Mercury. Journal of Geophysical Research, 2011, 116, n/a-n/a.	3.3	39
202	MESSENGER SciBox, An Automated Closed-loop Science Planning and Commanding System. , 2011, , .		0
203	The interplanetary magnetic field environment at Mercury's orbit. Planetary and Space Science, 2011, 59, 2075-2085.	0.9	35
204	The dayside magnetospheric boundary layer at Mercury. Planetary and Space Science, 2011, 59, 2037-2050.	0.9	33
205	Observations of suprathermal electrons in Mercury's magnetosphere during the three MESSENGER flybys. Planetary and Space Science, 2011, 59, 2016-2025.	0.9	31
206	The space environment of Mercury at the times of the second and third MESSENGER flybys. Planetary and Space Science, 2011, 59, 2066-2074.	0.9	28
207	MESSENGER observations of the plasma environment near Mercury. Planetary and Space Science, 2011, 59, 2004-2015.	0.9	78
208	Electron transport and precipitation at Mercury during the MESSENGER flybys: Implications for electron-stimulated desorption. Planetary and Space Science, 2011, 59, 2026-2036.	0.9	30
209	Reconstruction of propagating Kelvin–Helmholtz vortices at Mercury's magnetopause. Planetary and Space Science, 2011, 59, 2051-2057.	0.9	24
210	MESSENGER Observations of Transient Bursts of Energetic Electrons in Mercury's Magnetosphere. Science, 2011, 333, 1865-1868.	6.0	35
211	MESSENGER Observations of the Spatial Distribution of Planetary Ions Near Mercury. Science, 2011, 333, 1862-1865.	6.0	102
212	The Global Magnetic Field of Mercury from MESSENGER Orbital Observations. Science, 2011, 333, 1859-1862.	6.0	301
213	Comparison of the observed dependence of large-scale Birkeland currents on solar wind parameters with that obtained from global simulations. Annales Geophysicae, 2011, 29, 1809-1826.	0.6	21
214	Characteristics of the terrestrial field-aligned current system. Annales Geophysicae, 2011, 29, 1713-1729.	0.6	54
215	Mercury's magnetospheric magnetic field after the first two MESSENGER flybys. Icarus, 2010, 209, 23-39.	1.1	110
216	Whole-disk spectrophotometric properties of Mercury: Synthesis of MESSENGER and ground-based observations. Icarus, 2010, 209, 101-124.	1.1	35

#	Article	IF	CITATIONS
217	The Magnetic Field of Mercury. Space Science Reviews, 2010, 152, 307-339.	3.7	94
218	Magnetic field investigation of Mercury's magnetosphere and the inner heliosphere by MMO/MGF. Planetary and Space Science, 2010, 58, 279-286.	0.9	29
219	Modeling of the magnetosphere of Mercury at the time of the first MESSENGER flyby. Icarus, 2010, 209, 3-10.	1.1	67
220	Mercury's magnetosphere–solar wind interaction for northward and southward interplanetary magnetic field: Hybrid simulation results. Icarus, 2010, 209, 11-22.	1.1	66
221	Statistical analysis of the dependence of large-scale Birkeland currents on solar wind parameters. Annales Geophysicae, 2010, 28, 515-530.	0.6	45
222	MESSENGER Observations of Extreme Loading and Unloading of Mercury's Magnetic Tail. Science, 2010, 329, 665-668.	6.0	172
223	Mercury's Complex Exosphere: Results from MESSENGER's Third Flyby. Science, 2010, 329, 672-675.	6.0	70
224	MESSENGER observations of large flux transfer events at Mercury. Geophysical Research Letters, 2010, 37, .	1.5	57
225	Empirical modeling of a CIRâ€driven magnetic storm. Journal of Geophysical Research, 2010, 115, .	3.3	38
226	Rapid scattering of radiation belt electrons by stormâ€ŧime EMIC waves. Geophysical Research Letters, 2010, 37, .	1.5	135
227	Observations of Kelvinâ€Helmholtz waves along the duskâ€side boundary of Mercury's magnetosphere during MESSENGER's third flyby. Geophysical Research Letters, 2010, 37, .	1.5	50
228	Observations of ion cyclotron waves in the solar wind near 0.3 AU. Journal of Geophysical Research, 2010, 115, .	3.3	70
229	Seasonal and interplanetary magnetic field dependence of the field-aligned currents for both Northern and Southern Hemispheres. Annales Geophysicae, 2009, 27, 1701-1715.	0.6	60
230	MESSENGER Observations of Magnetic Reconnection in Mercury's Magnetosphere. Science, 2009, 324, 606-610.	6.0	234
231	Mercury's internal magnetic field: Constraints on large- and small-scale fields of crustal origin. Earth and Planetary Science Letters, 2009, 285, 340-346.	1.8	22
232	Modeling Mercury's internal magnetic field with smooth inversions. Earth and Planetary Science Letters, 2009, 285, 328-339.	1.8	41
233	MESSENGER and Venus Express observations of the solar wind interaction with Venus. Geophysical Research Letters, 2009, 36, .	1.5	37
234	Upstream conditions at Mercury during the first MESSENGER flyby: Results from two independent solar wind models. Geophysical Research Letters, 2009, 36, .	1.5	3

#	Article	IF	CITATIONS
235	Comparison of ultra″owâ€frequency waves at Mercury under northward and southward IMF. Geophysical Research Letters, 2009, 36, .	1.5	17
236	Space environment of Mercury at the time of the first MESSENGER flyby: Solar wind and interplanetary magnetic field modeling of upstream conditions. Journal of Geophysical Research, 2009, 114, .	3.3	37
237	The MESSENGER Science Planning and Commanding System. , 2009, , .		4
238	Comprehensive Mission Simulation Contingency Analyses: Achieving Science Observation Plan Resiliency by Design. , 2009, , .		2
239	Narrowâ€band ultraâ€lowâ€frequency wave observations by MESSENGER during its January 2008 flyby through Mercury's magnetosphere. Geophysical Research Letters, 2009, 36, .	1.5	26
240	MESSENGER observations of Mercury's magnetosphere during northward IMF. Geophysical Research Letters, 2009, 36, .	1.5	55
241	Kinetic instabilities in Mercury's magnetosphere: Threeâ€dimensional simulation results. Geophysical Research Letters, 2009, 36, .	1.5	38
242	Modeling the response of the induced magnetosphere of Venus to changing IMF direction using MESSENGER and Venus Express observations. Geophysical Research Letters, 2009, 36, .	1.5	9
243	A solar storm observed from the Sun to Venus using the STEREO, Venus Express, and MESSENGER spacecraft. Journal of Geophysical Research, 2009, 114, .	3.3	65
244	The Magnetic Field of Mercury. Space Sciences Series of ISSI, 2009, , 307-339.	0.0	2
245	Controlling factors of Region 2 field-aligned current and its relationship to the ring current: Model results. Advances in Space Research, 2008, 41, 1234-1242.	1.2	3
246	Magnetic field line curvature induced pitch angle diffusion in the inner magnetosphere. Journal of Geophysical Research, 2008, 113, .	3.3	45
247	Highâ€latitude ionosphere convection and Birkeland current response for the 15 May 2005 magnetic storm recovery phase. Journal of Geophysical Research, 2008, 113, .	3.3	18
248	Mercury's Magnetosphere After MESSENGER's First Flyby. Science, 2008, 321, 85-89.	6.0	166
249	The Structure of Mercury's Magnetic Field from MESSENGER's First Flyby. Science, 2008, 321, 82-85.	6.0	194
250	Global observations of electromagnetic and particle energy flux for an event during northern winter with southward interplanetary magnetic field. Annales Geophysicae, 2008, 26, 1415-1430.	0.6	11
251	Statistical Birkeland current distributions from magnetic field observations by the Iridium constellation. Annales Geophysicae, 2008, 26, 671-687.	0.6	132
252	Comparison of Birkeland current observations during two magnetic cloud events with MHD simulations. Annales Geophysicae, 2008, 26, 499-516.	0.6	17

#	Article	IF	CITATIONS
253	Technique: Large-scale ionospheric conductance estimated from combined satellite and ground-based electromagnetic data. Journal of Geophysical Research, 2007, 112, n/a-n/a.	3.3	21
254	MESSENGER: Exploring Mercury's Magnetosphere. Space Science Reviews, 2007, 131, 133-160.	3.7	55
255	The Magnetometer Instrument on MESSENGER. Space Science Reviews, 2007, 131, 417-450.	3.7	254
256	Impact of ULF oscillations in solar wind dynamic pressure on the outer radiation belt electrons. Geophysical Research Letters, 2006, 33, .	1.5	61
257	Relationship between Region 2 field-aligned current and the ring current: Model results. Journal of Geophysical Research, 2006, 111, .	3.3	24
258	Storm time evolution of the outer radiation belt: Transport and losses. Journal of Geophysical Research, 2006, 111, .	3.3	155
259	Comparison of large-scale Birkeland currents determined from Iridium and SuperDARN data. Annales Geophysicae, 2006, 24, 941-959.	0.6	27
260	Comparison of Interplanetary Disturbances at theNEARSpacecraft with Coronal Mass Ejections at the Sun. Astrophysical Journal, 2005, 621, 524-536.	1.6	35
261	Neutral composition effects on ionospheric storms at middle and low latitudes. Journal of Geophysical Research, 2005, 110, .	3.3	42
262	High-latitude electromagnetic and particle energy flux during an event with sustained strongly northward IMF. Annales Geophysicae, 2005, 23, 1295-1310.	0.6	31
263	On the source of Pc1-2 waves in the plasma mantle. Journal of Geophysical Research, 2005, 110, .	3.3	16
264	Impact of toroidal ULF waves on the outer radiation belt electrons. Journal of Geophysical Research, 2005, 110, .	3.3	72
265	Storm time dawn-dusk asymmetry of the large-scale Birkeland currents. Journal of Geophysical Research, 2005, 110, .	3.3	39
266	High-latitude poynting flux from combined Iridium and SuperDARN data. Annales Geophysicae, 2004, 22, 2861-2875.	0.6	34
267	IMAGE/HENA: pressure and current distributions during the 1 October 2002 storm. Advances in Space Research, 2004, 33, 719-722.	1.2	32
268	Determination of the properties of Mercury's magnetic field by the MESSENGER mission. Planetary and Space Science, 2004, 52, 733-746.	0.9	61
269	Conditions governing localized high-latitude dayside aurora. Geophysical Research Letters, 2004, 31, .	1.5	12
270	Data-derived forecasting model for relativistic electron intensity at geosynchronous orbit. Geophysical Research Letters, 2004, 31, n/a-n/a.	1.5	44

#	Article	IF	CITATIONS
271	Intercomparison of ionospheric electrodynamics from the Iridium constellation with global MHD simulations. Journal of Geophysical Research, 2004, 109, .	3.3	35
272	Radial Variation of Magnetic Flux Ropes: Case Studies with ACE and NEAR. AIP Conference Proceedings, 2003, , .	0.3	3
273	Empirical model for μ scattering caused by field line curvature in a realistic magnetosphere. Journal of Geophysical Research, 2002, 107, SMP 3-1.	3.3	43
274	Birkeland current system key parameters derived from Iridium observations: Method and initial validation results. Journal of Geophysical Research, 2002, 107, SMP 11-1.	3.3	91
275	Observations of two types of Pc 1-2 pulsations in the outer dayside magnetosphere. Journal of Geophysical Research, 2002, 107, SMP 20-1-SMP 20-20.	3.3	99
276	Detection of ultralow-frequency cavity modes using spacecraft data. Journal of Geophysical Research, 2002, 107, SMP 7-1.	3.3	52
277	Estimation of global field aligned currents using the iridium® System magnetometer data. Geophysical Research Letters, 2001, 28, 2165-2168.	1.5	187
278	Multiple spacecraft flux rope modeling of the Bastille Day magnetic cloud. Geophysical Research Letters, 2001, 28, 4417-4420.	1.5	27
279	The MESSENGER mission to Mercury: scientific payload. Planetary and Space Science, 2001, 49, 1467-1479.	0.9	118
280	Sensing global Birkeland currents with iridium® engineering magnetometer data. Geophysical Research Letters, 2000, 27, 4045-4048.	1.5	222
281	Intercomparison of NEAR and Wind interplanetary coronal mass ejection observations. Journal of Geophysical Research, 1999, 104, 28217-28223.	3.3	43
282	Onset of nonadiabatic particle motion in the near-Earth magnetotail. Journal of Geophysical Research, 1997, 102, 17553-17569.	3.3	54
283	The diffuse aurora: A significant source of ionization in the middle atmosphere. Journal of Geophysical Research, 1997, 102, 28203-28214.	3.3	75
284	The NEAR magnetic field investigation: Science objectives at asteroid Eros 433 and experimental approach. Journal of Geophysical Research, 1997, 102, 23751-23759.	3.3	26
285	Electron and ion signatures of field line topology at the low-shear magnetopause. Journal of Geophysical Research, 1997, 102, 4847-4863.	3.3	100
286	Near Magnetic Field Investigation, Instrumentation, Spacecraft Magnetics and Data Access. Space Science Reviews, 1997, 82, 255-281.	3.7	18
287	Magnetic impulse events and associated Pc 1 bursts at dayside high latitudes. Journal of Geophysical Research, 1996, 101, 7793-7799.	3.3	32
288	Source region of 0.2 to 1.0 Hz geomagnetic pulsation bursts. Geophysical Research Letters, 1996, 23, 769-772.	1.5	39

#	Article	IF	CITATIONS
289	On determining polarization characteristics of ion cyclotron wave magnetic field fluctuations. Journal of Geophysical Research, 1996, 101, 13195-13213.	3.3	52
290	Observational test of local proton cyclotron instability in the Earth's magnetosphere. Journal of Geophysical Research, 1996, 101, 21527-21543.	3.3	134
291	Effects of wave superposition on the polarization of electromagnetic ion cyclotron waves. Journal of Geophysical Research, 1996, 101, 24869-24885.	3.3	46
292	Proton cyclotron wave-ion interactions observed by AMPTE/CCE. Geophysical Monograph Series, 1995, , 193-200.	0.1	2
293	Particle signatures of magnetic topology at the magnetopause: AMPTE/CCE observations. Journal of Geophysical Research, 1995, 100, 11805.	3.3	88
294	Ion Anisotropy-driven waves in the Earth's magnetosheath and plasma depletion layer. Geophysical Monograph Series, 1994, , 111-119.	0.1	8
295	A limited closure relation for anisotropic plasmas from the Earth's magnetosheath*. Physics of Plasmas, 1994, 1, 1676-1683.	0.7	54
296	Low-frequency magnetic fluctuation spectra in the magnetosheath and plasma depletion layer. Journal of Geophysical Research, 1994, 99, 5893.	3.3	49
297	Magnetic spectral signatures in the Earth's magnetosheath and plasma depletion layer. Journal of Geophysical Research, 1994, 99, 5877.	3.3	229
298	Freja's contribution to the ISTP event of October 27, 1992. A distorted magnetosphere. Geophysical Research Letters, 1994, 21, 1871-1874.	1.5	1
299	Ionospheric currents correlated with geomagnetic induced currents; Freja magnetic field measurements and the Sunburst Monitor System. Geophysical Research Letters, 1994, 21, 1867-1870.	1.5	14
300	Bounded anisotropy fluid model for ion temperatures. Journal of Geophysical Research, 1994, 99, 11225.	3.3	98
301	Ion anisotropy instabilities in the magnetosheath. Journal of Geophysical Research, 1993, 98, 1481-1488.	3.3	168
302	Auroral currents during the magnetic storm of November 8 and 9, 1991: Observations from the Upper Atmosphere Research Satellite Particle Environment Monitor. Geophysical Research Letters, 1993, 20, 1327-1330.	1.5	19
303	Ion anisotropies in the magnetosheath. Geophysical Research Letters, 1993, 20, 1767-1770.	1.5	50
304	Electromagnetic ion cyclotron waves stimulated by modest magnetospheric compressions. Journal of Geophysical Research, 1993, 98, 11369-11382.	3.3	212
305	Electromagnetic ion cyclotron waves in the plasma depletion layer. Journal of Geophysical Research, 1993, 98, 13477-13490.	3.3	46
306	The UARS particle environment monitor. Journal of Geophysical Research, 1993, 98, 10649-10666.	3.3	52

#	Article	IF	CITATIONS
307	A statistical study of Pc 1–2 magnetic pulsations in the equatorial magnetosphere: 1. Equatorial occurrence distributions. Journal of Geophysical Research, 1992, 97, 3075-3088.	3.3	389
308	A statistical study of Pc 1–2 magnetic pulsations in the equatorial magnetosphere: 2. Wave properties. Journal of Geophysical Research, 1992, 97, 3089-3101.	3.3	220
309	Electromagnetic ion cyclotron waves observed in the plasma depletion layer. Geophysical Research Letters, 1991, 18, 1955-1958.	1.5	105
310	Pc1 pulsations observed by AMPTE/CCE in the Earth's outer magnetosphere. Geophysical Research Letters, 1990, 17, 1853-1856.	1.5	42
311	A statistical study of Pc 3–5 pulsations observed by the AMPTE/CCE Magnetic Fields Experiment, 1. Occurrence distributions. Journal of Geophysical Research, 1990, 95, 10495-10523.	3.3	226
312	Propagation of Compressional Pc 3 Pulsations from Space to the Ground: A Case Study Using Multipoint Measurements. Geophysical Monograph Series, 0, , 355-363.	0.1	20
313	Proton Anisotropies Upstream of the Magnetopause. Geophysical Monograph Series, 0, , 123-129.	0.1	4